Supporting Information

A general strategy to in-situ synthesize hollow metal sulfide/MOF heterostructure for high performance supercapacitor

Yingchao Wang,[a] Guochang Li,*[,a] Jiachao Zhou,[a] Kai Tao,[a] Wenna Zhao,[b] Linli Chen,[a] Lei Han*[,a]

[a]State Key Laboratory Base of Novel Functional Materials and Preparation Science, School of Materials Science and Chemical Engineering, Ningbo University, Ningbo, Zhejiang 315211, China.

[b]School of Biological and Chemical Engineering, Ningbotech University, Ningbo, Zhejiang 315100, China.

*Corresponding authors.

E-mail: liguochang@nbu.edu.cn (G. Li); hanlei@nbu.edu.cn (L. Han)

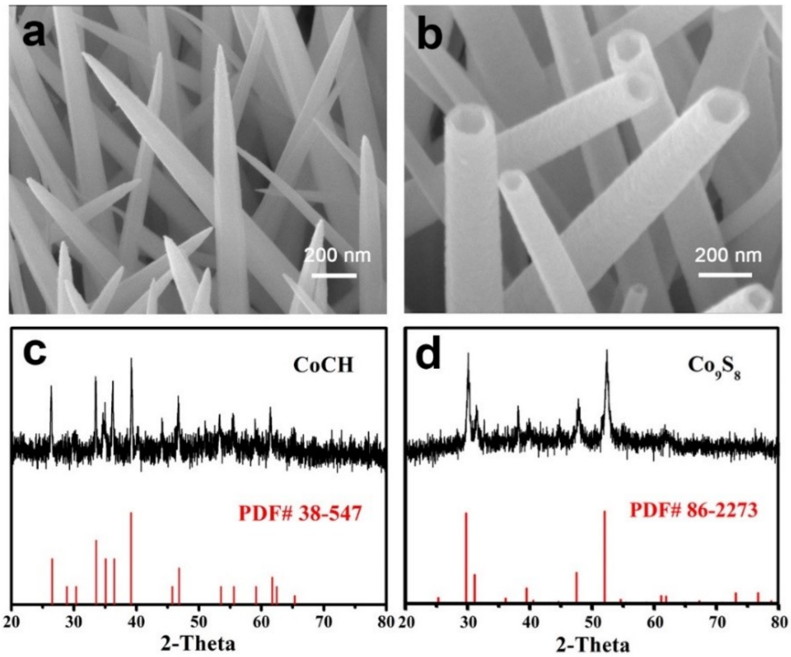

Figure S1. SEM images (a,b) and XRD patterns (c,d) of CoCH and Co_9S_8. (a,c) CoCH; (b,d) Co_9S_8

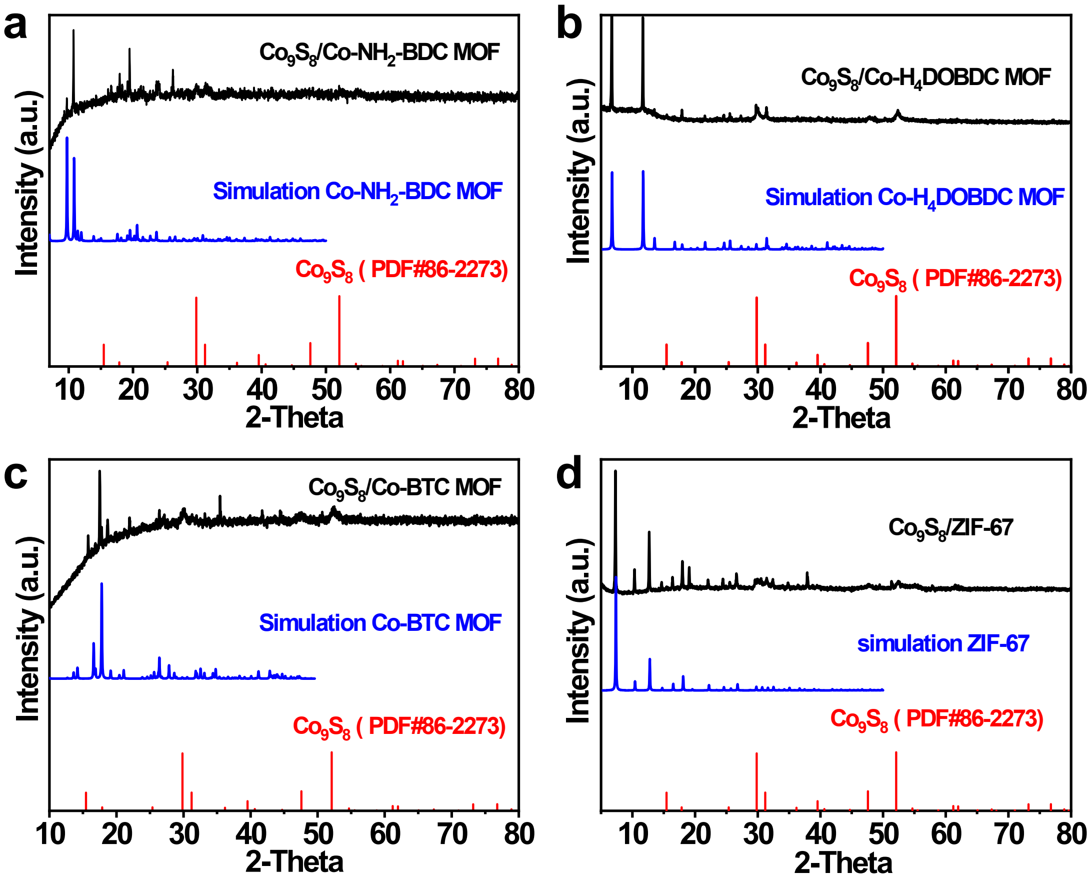

Figure S2. XRD patterns of the Co_9S_8/MOF. (a) Co_9S_8/Co-NH_2-BDC MOF; (b) Co_9S_8/Co-H_4DOBDC MOF; (c) Co_9S_8/Co-BTC MOF; (d) Co_9S_8/ ZIF-67.

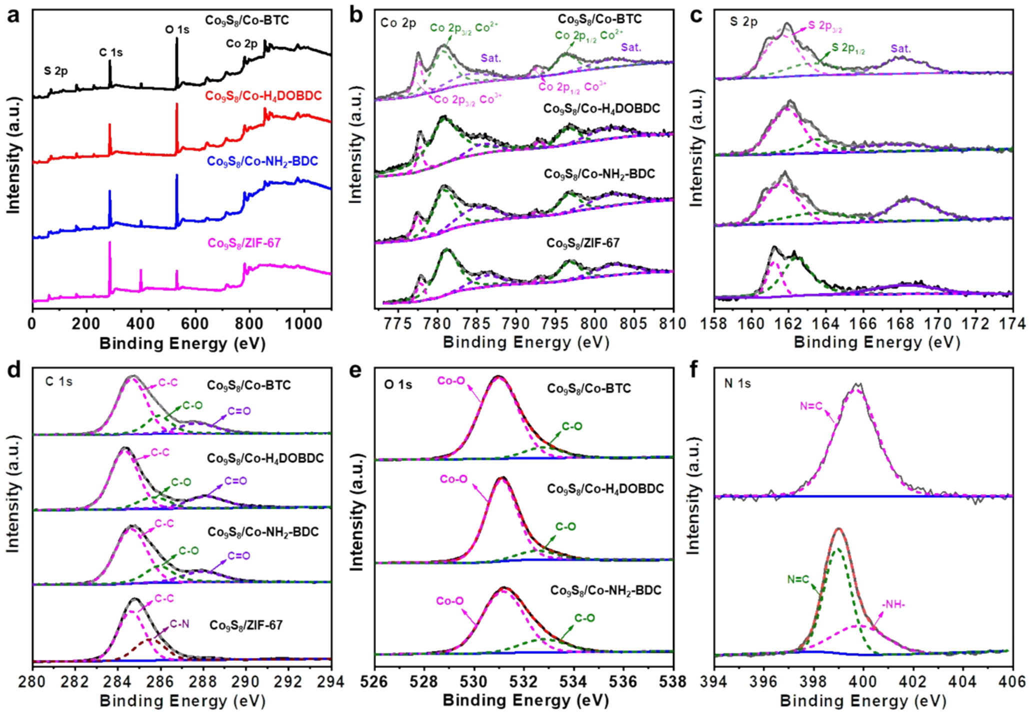

Figure S3. XPS spectrum of the Co_9S_8/MOF. (a) survey spectrum; (b) Co 2p; (c) S 2p (d) C 1s; (e) O 1s; (f) N 1s.

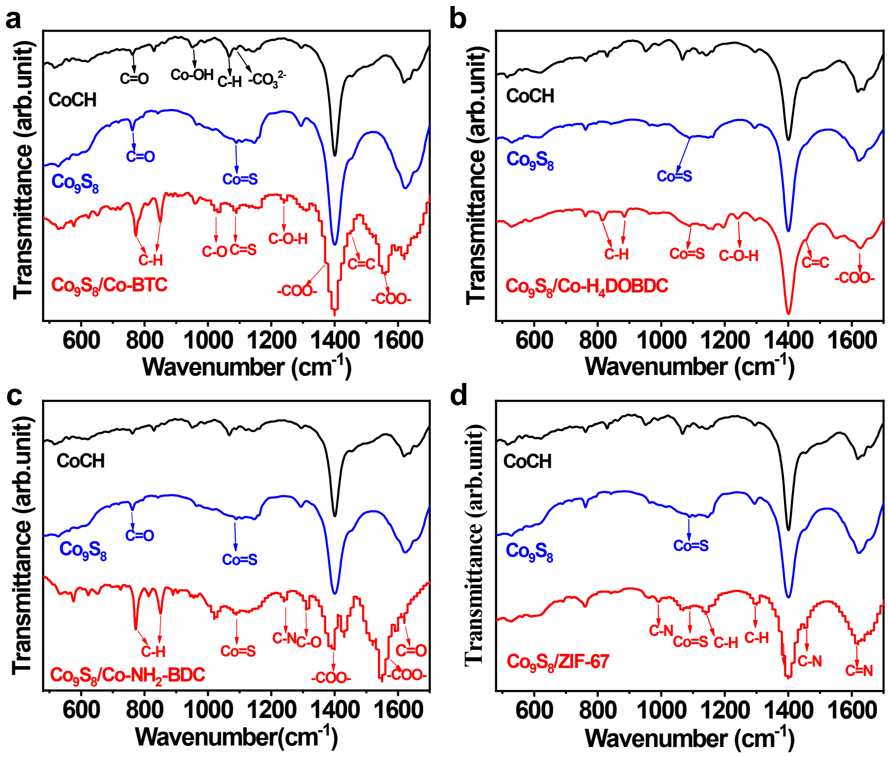

Figure S4. FTIR spectrum of the CoCH, Co_9S_8 and Co_9S_8/MOF. (a) Co_9S_8/Co-BTC MOF; (b) Co_9S_8/Co-H_4DOBDC MOF; (c) Co_9S_8/Co-NH_2-BDC MOF; (d) Co_9S_8/ZIF-67.

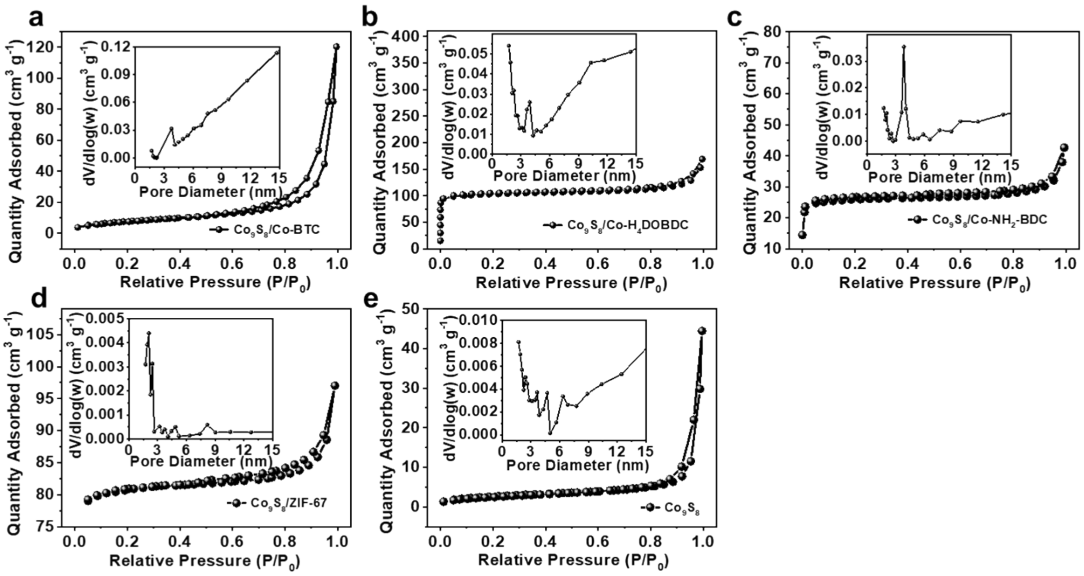

Figure S5. N_2 adsorption-desorption isotherm and pore distribution curve of the Co_9S_8/MOF and Co_9S_8. (a) Co_9S_8/Co-BTC MOF; (b) Co_9S_8/Co-H_4DOBDC MOF; (c) Co_9S_8/Co-NH_2-BDC MOF; (d) Co_9S_8/ZIF-67; (e) Co_9S_8.

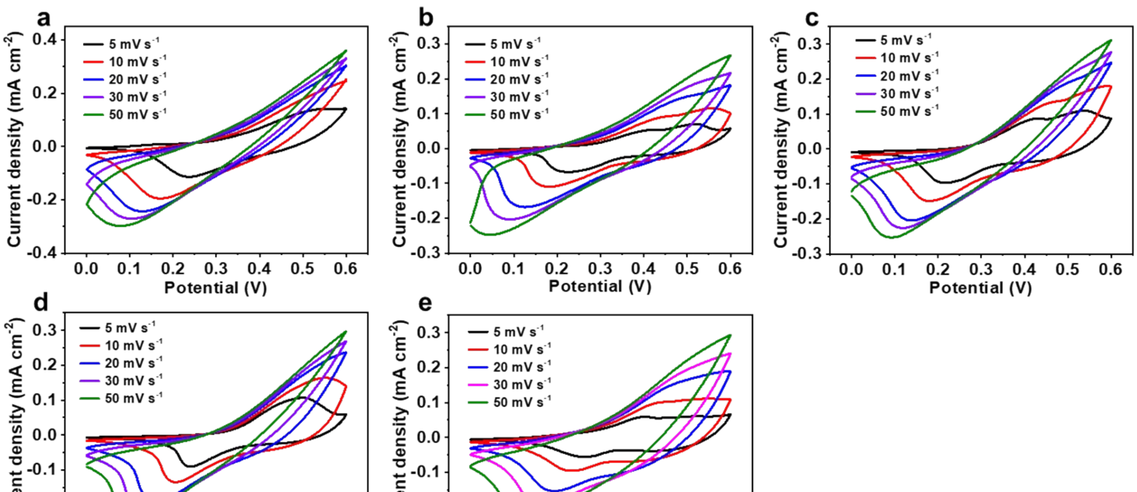

Figure S6. CV curves of the Co_9S_8/MOF at different scan rates. (a) Co_9S_8/Co-BDC MOF; (b) Co_9S_8/Co-NH_2-BDC MOF; (c) Co_9S_8/Co-H_4DOBDC MOF; (d) Co_9S_8/Co-BTC MOF; (e) Co_9S_8/ZIF-67.

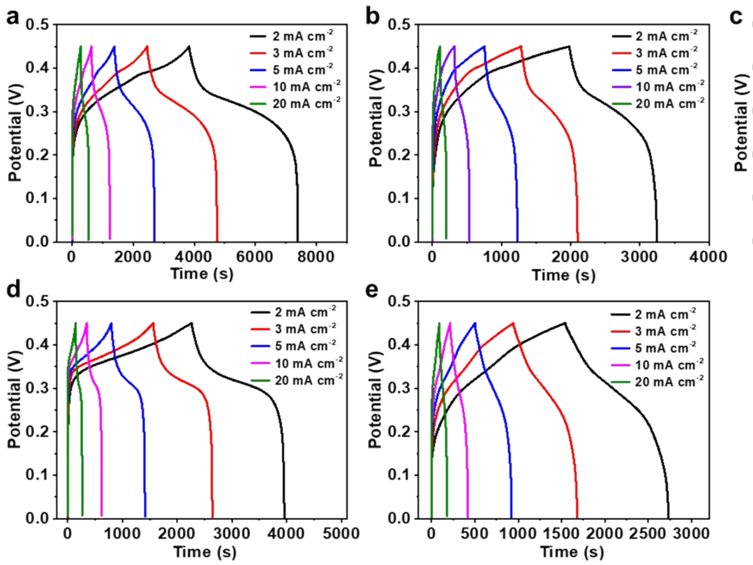

Figure S7. CP curves of the Co_9S_8/MOFs at different current densities. (a) Co_9S_8/Co-BDC MOF; (b) Co_9S_8/Co-NH_2-BDC MOF; (c) Co_9S_8/Co-H_4DOBDC MOF; (d) Co_9S_8/Co-BTC MOF; (e) Co_9S_8/ZIF-67.

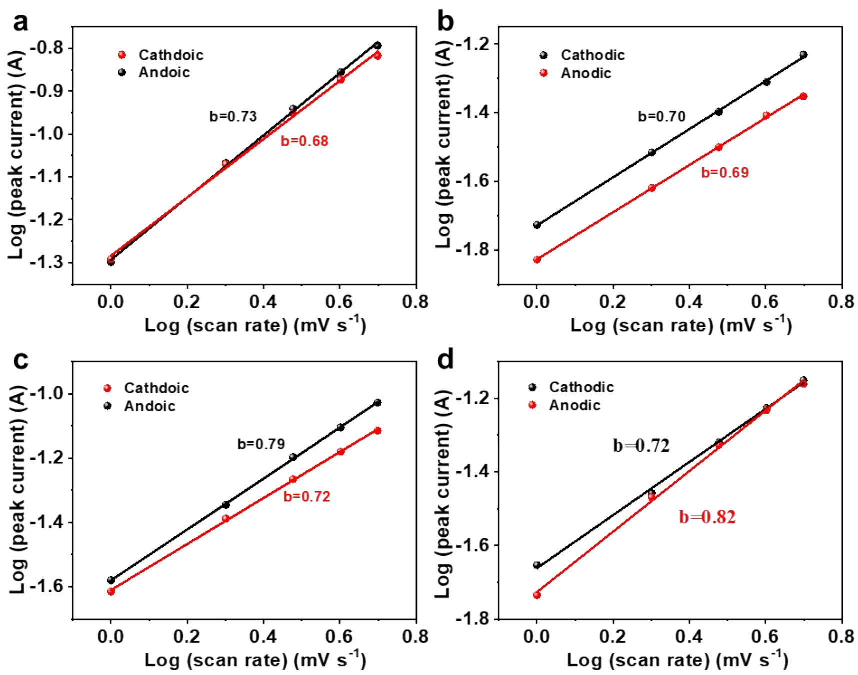

Figure S8. Plot of υ versus $υ^{1/2}$ and b value of the Co_9S_8/MOF. (a) Co_9S_8/Co-NH_2-BDC MOF; (b) Co_9S_8/Co-H_4DOBDC MOF; (c) Co_9S_8/Co-BTC MOF; (d) Co_9S_8/ZIF-67.

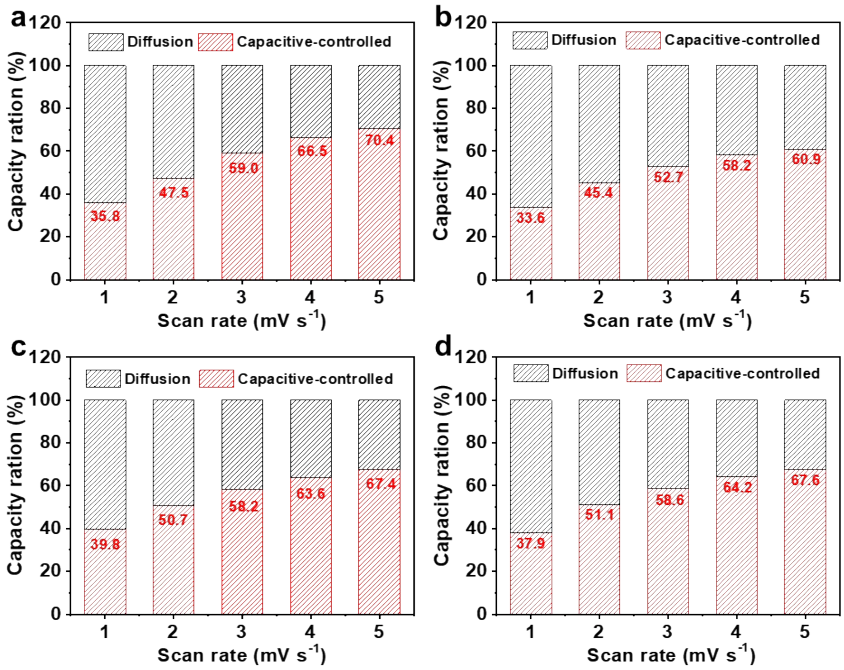

Figure S9. Calculated capacitive- and diffusion-controlled contribution of the Co_9S_8/MOF. (a) Co_9S_8/Co-NH_2-BDC MOF; (b) Co_9S_8/Co-H_4DOBDC MOF; (c) Co_9S_8/Co-BTC MOF; (d) Co_9S_8/ ZIF-67.

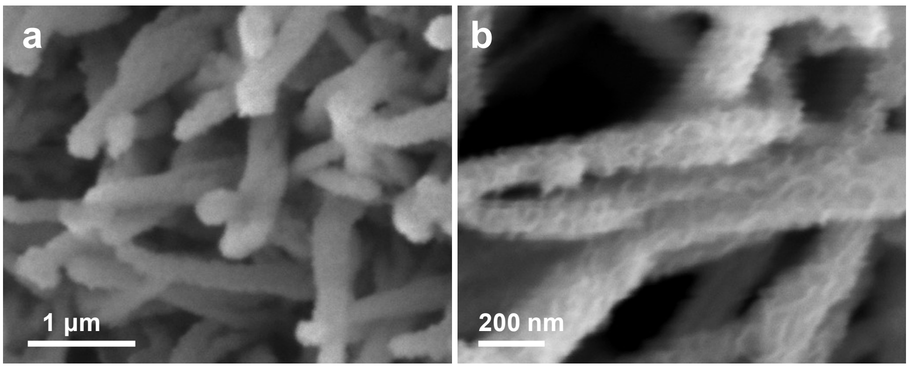

Figure S10. The SEM iamges of Co_9S_8/Co-BDC after the electrochemical test.

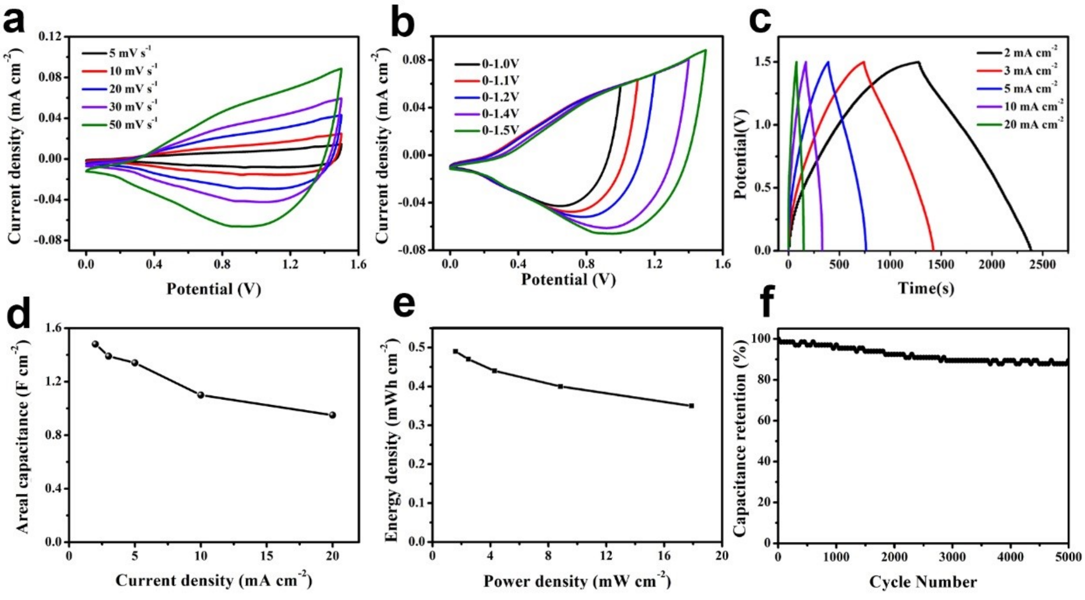

Figure S11. The electrochemical performance of Co_9S_8/Co-NH_2-BDC MOF//AC ASC in 2 mol L^{-1} KOH electrolyte. (a) CV curves at different scan rates; (b) CV curves at different potential; (c) GCD curves at different current densities; (d) Areal capacitance; (e) Energy density and power density; (f) Cycling performance.

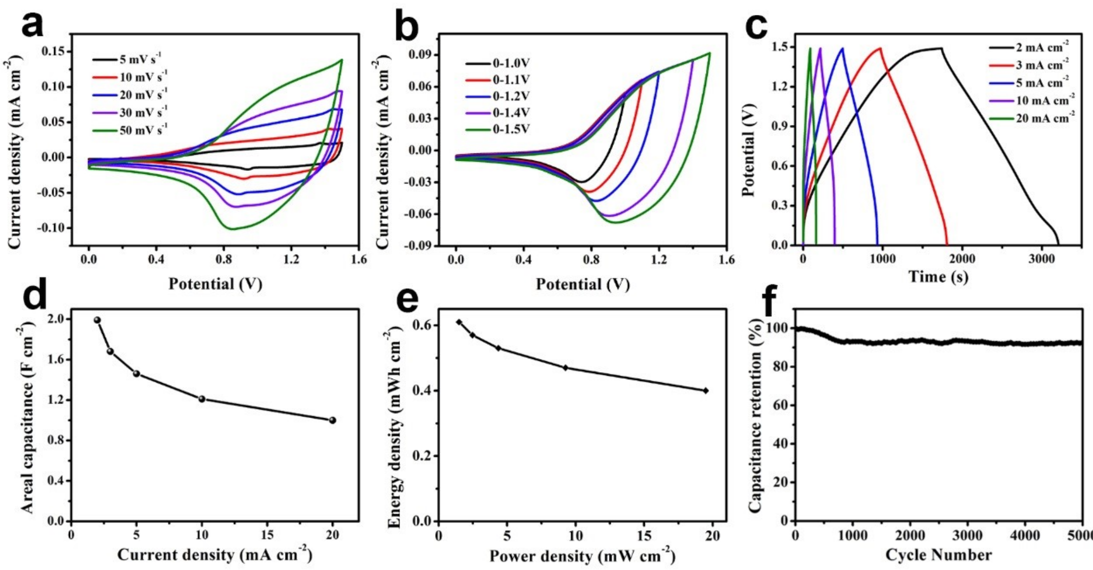

Figure S12. The electrochemical performance of Co_9S_8/Co-H_4DOBDC MOF//AC ASC in 2 mol L^{-1} KOH electrolyte. (a) CV curves at different scan rates; (b) CV curves at different potential; (c) GCD curves at different current densities; (d) Areal capacitance; (e) Energy density and power density; (f) Cycling performance.

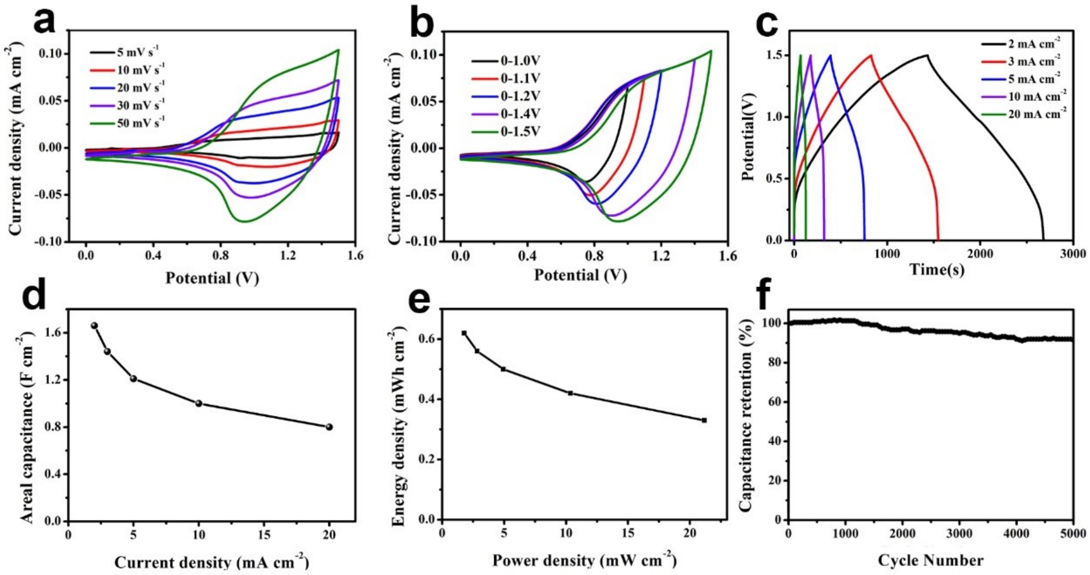

Figure S13. The electrochemical performance of Co_9S_8/Co-BTC MOF//AC ASC in 2 mol L^{-1} KOH electrolyte. (a) CV curves at different scan rates; (b) CV curves at different potential; (c) GCD curves at different current densities; (d) Areal capacitance; (e) Energy density and power density; (f) Cycling performance.

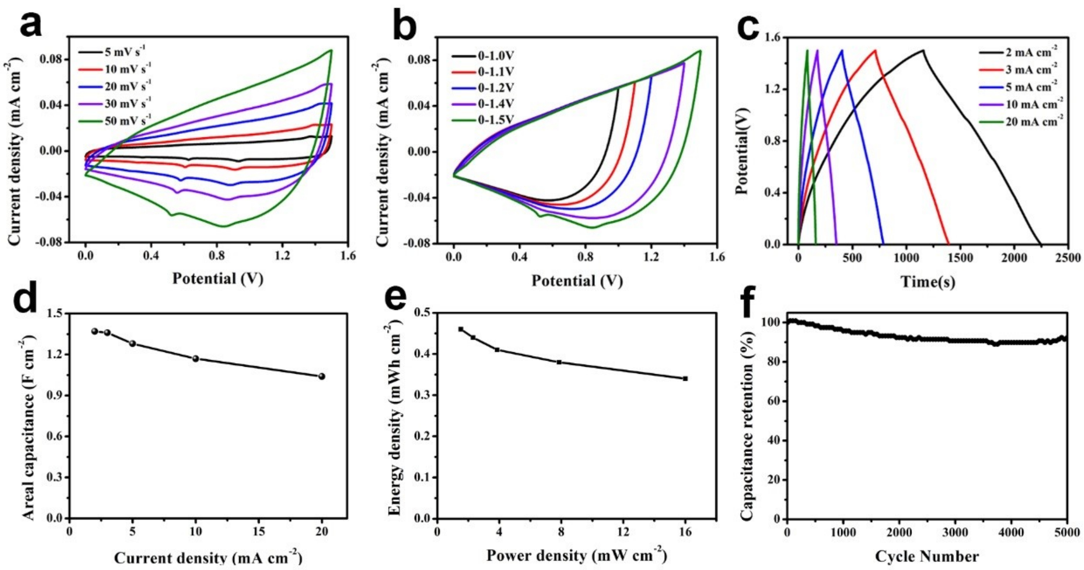

Figure S14. The electrochemical performance of Co_9S_8/ZIF-67//AC ASC in 2 mol L^{-1} KOH electrolyte. (a) CV curves at different scan rates; (b) CV curves at different potential; (c) GCD curves at different current densities; (d) Areal capacitance; (e) Energy density and power density; (f) Cycling performance.

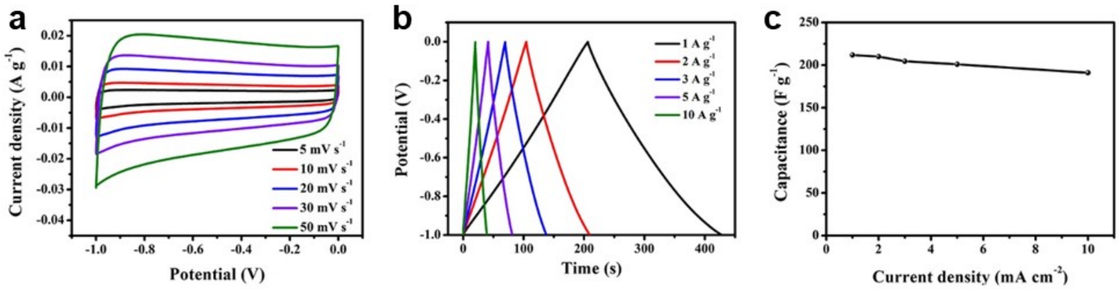

Figure S15. The electrochemical performance of AC in 2 mol L^{-1} KOH electrolyte. (a) CV curves; (b) GCD curves; (c) Capacitances versus current densities.

Table S1 The electrochemical performance of CoCH, Co_9S_8 and Co_9S_8/MOF in three-electrode system.

Electrode material	Specific capacity	Specific capacitance	Cycle performance	R_s/R_{ct}
CoCH	126.4 mAh cm^{-2}	1.01F cm^{-2} (0.455C cm^{-2})	68.60%	0.8957/1.052
Co_9S_8	537.8 mAh cm^{-2}	4.30F cm^{-2}(1.94C cm^{-2})	71.33%	0.8316/0.219
Co_9S_8/Co-BDC MOF	1980.0 mAh cm^{-2}	15.84F cm^{-2}(4.53C cm^{-2})	87.50%	0.74111/0.057
Co_9S_8/Co-NH_2-BDC MOF	702.3 mAh cm^{-2}	5.62F cm^{-2}(7.13C cm^{-2})	93.44%	0.54321/0.1006
Co_9S_8/Co-H_4DOBDC MOF	1257.5 mAh cm^{-2}	10.06F cm^{-2}(2.33C cm^{-2})	98.28%	0.6761/0.216
Co_9S_8/Co-BTC MOF	938.9 mAh cm^{-2}	7.51F cm^{-2}(3.38C cm^{-2})	83.92%	0.6162/0.2122
Co_9S_8/ZIF-67	661.1 mAh cm^{-2}	5.29F cm^{-2}(2.38C cm^{-2})	91.89%	0.6256/0.2129

Table S2 The electrochemical performance of the Co_9S_8/MOFs//AC ASC

ASC	**Specific capacitance**	**Energy density**	**Power density**	**Cycle performance**
Co_9S_8/Co-BDC MOF//AC	2.49 F cm^{-2}	0.87 mWh cm^{-2}	1.68 mW cm^{-2}	95.44%
Co_9S_8/Co-NH_2-BDC MOF//AC	1.66 F cm^{-2}	0.62 mWh cm^{-2}	1.78 mW cm^{-2}	89.39%
Co_9S_8/Co-H_4DOBDC MOF//AC	1.99 F cm^{-2}	0.61 mWh cm^{-2}	1.48 mW cm^{-2}	92.48%
Co_9S_8/Co-BTC MOF//AC	1.48 F cm^{-2}	0.49 mWh cm^{-2}	1.59 mW cm^{-2}	91.53%
Co_9S_8/ZIF-67//AC	1.37 F cm^{-2}	0.46 mWh cm^{-2}	1.52 mW cm^{-2}	92.37%